The influence of transition metals on the electronic structure of ZnSe host crystal: fundamental reflectivity analysis

1997 J. Phys.: Condens. Matter 9 8767

(http://iopscience.iop.org/0953-8984/9/41/020)

J. Phys.: Condens. Matter **9** (1997) 8767–8786. Printed in the UK PII: S0953-8984(97)80257-3

The influence of transition metals on the electronic structure of ZnSe host crystal: fundamental reflectivity analysis

A Kisiel†, M Piacentini‡, D Dębowska†, N Zema§, F Lama§, M Zimnal-Starnawska†, W Giriat‖, A Hołda† and R Markowski†¶

† Instytut Fizyki, Uniwersytet Jagielloński, Kraków, Poland
‡ Dipartimento di Energetica, Universitá degli Studi di Roma 'La Sapienza', Roma, Italy
§ Istituto di Stuttura della Materia del CNR, Frascati, Italy
‖ Istituto Venezolano Investigazione Cientifica, Centro de Fisica, Caracas, Venezuela

Received 11 December 1996, in final form 2 June 1997

Abstract. The optical properties of the semiconducting compounds $Zn_{1-x}Me_xSe$ (Me = Ti, V, Cr, Mn, Fe, Co, and Ni) crystallizing in the zinc-blende structure have been investigated. Reflectivity spectra of these materials have been taken at room and liquid nitrogen temperatures. The measurements have been performed in the 4–25 eV energy range using synchrotron radiation from the ADONE storage ring in Frascati. Comparisons between the reflectivity spectra of the ternary systems and those of the host crystal ZnSe have been made, and models explaining the influence of the transition metal ions on the electronic structure of the host crystal ZnSe have been discussed.

1. Introduction

Semimagnetic semiconductors, also known as diluted magnetic semiconductors (DMSs), are alloys of the II–VI family of semiconductors, in which the group-II-element cations are randomly replaced by transition metal (TM) cations, while the crystal structure of the host crystal is maintained. TM-doped II–VI semimagnetic semiconductors have attracted considerable attention in the last fifteen years [1]. Besides the well-known changes in the electronic band structure of ordinary ternary semiconducting compounds due to changes in composition, the DMSs show novel magneto-optical and magneto-transport properties. In this context the interaction between the TM 3d electrons and the electronic states of the host crystal is of special interest. The introduction of ions with large magnetic moments leads to a number of magnetic phenomena, which have been the focus of many studies (see for instance reference [2]). Since the $4s^2$ electrons of the magnetic ion contribute to bonding in the same fashion as the two outer s electrons of the group-II element, the crystal-field-split manifold of d levels plays a major role in the optical and electronic properties of DMSs. The existence of a large exchange interaction between the valence band electrons and the TM-ion 3d electrons, the so-called s, p–d interaction, leads to the d-electron wavefunctions being more extended. As is evident from the impurity spin moment, the 3d ions have a strong intra-ion Coulomb correlation [3]. Thus correlations, together with the high degree

¶ Permanent address: Syracuse University, Northeast Parallel, Architectures Center, 11 College Place, Syracuse, NY 13244-4100, USA.

0953-8984/97/418767+20$19.50

of spatial disorder introduced by the random substitution of 3d ions, can lead to some localized electronic states. Hence, in contrast to the shallow-donor case, the insulator-to-metal transition will be inhibited even when impurity band formation occurs.

Recently some optical studies [4–9] as well as photoemission [10, 11] and magnetic measurements [12] of ZnMeSe (Me = Mn, Fe, Co, Cr) have been performed in order to work out the influence of the presence of TM on the host crystal properties. Hence in this field there is a growing interest in ZnSe materials doped with TMs such as Ti, V, Cr, Co, and Ti, because of their sometimes extraordinary properties.

The aim of this paper is to present in a systematic way fundamental reflectivity studies which are a probe of the interaction of the different TMs with ZnSe band structure. For these purposes we performed reflectivity studies on ZnMeSe ternary compounds with Me = Mn, Fe, Co, Ni, Cr, V, and Ti. This type of study allows us to develop and analyse models of the interaction of the 3d open-shell electrons of the TMs, and their effect on the valence band and conduction band structure of ZnSe. It is important to discuss the variation in the relative intensities as well as the shifts in energy position of the main reflectivity structures that occur on adding different TMs. Such systematic optical and photoemission studies have been reported for cadmium tellurides and selenides with Mn [13–17] and Fe [18–22], and some work has been done also on zinc selenide ternary compounds [4–11]. Work to date on these DMS systems has been largely concentrated on the Mn-, Fe-, and Co-doped semiconductors, and the results are summarized in several reviews [2, 23]. For these compounds some magnetic and optical results have been obtained using optical methods, which give some information about d–d intra-gap transitions. Some near- and far-IR absorption spectra [24] as well as absorption measurements of Ni-based ZnSe [6] have been obtained, confirming the expected d–d nickel transitions. In the case of ZnTiSe, some optical and electro-optical properties have been examined near the optical gap region, and the observed structures have been identified on the basis of theoretical calculations as Ti^{2+} multiplet transitions [8]. Also comprehensive photoacoustic studies have been performed on Fe- and Co-based ZnSe, providing information on d–d transitions [25, 26]. Almost no magnetic data are available and very little optical research has been done for ZnVSe [7], ZnNiSe [6, 24], and ZnTiSe [8]. However, in the case of Cr-doped ZnSe, quite a lot of magnetic measurements have been performed [12, 27, 28] with the aim of explaining the extraordinary ferromagnetic behaviour, compared with that of the other antiferromagnetically ordered TM-doped ZnSe compounds. Valence band splitting of ZnCrSe which is reversed relative to that of the antiferromagnetically ordered materials containing Mn, Co, or Fe has been observed, indicating the ferromagnetic p–d exchange in this material. On the other hand, Fe-based ZnMeSe shows the Van Vleck type of paramagnetism, and Mn- and Co-doped ZnSe exhibit the Brillouin type of paramagnetism [2].

2. Experiment

The reflectivity measurements were performed at room temperature (RT) and liquid nitrogen temperature at the vacuum ultraviolet beamline of PULS Laboratories at the INFN Frascati National Laboratories. Synchrotron radiation coming from the ADONE storage ring was focused onto the entrance slit of a 1 m near-normal-incidence monochromator equipped with two interchangeable gratings under vacuum conditions. A 1440 lines mm^{-1} gold-coated grating was used in the 10–30 eV photon energy range, and a 600 lines mm^{-1} ($Al + MgF_2$)-coated grating was used to cover the 4–10 eV photon energy range. The average energy resolution $\Delta E/E$ used for these measurements was better than 1×10^{-3} over the entire spectral range. Good-quality $Zn_{1-x}Me_xSe$ (Me = Mn, Fe, Co, Ni, Cr, V, and

Ti) single crystals with different nominal concentrations of transition metals were cleaved before being mounted inside the reflectometer from ingots grown using chemical vapour transport (CVT) with I_2 as a carrier medium [29]. The quality of the samples was checked by x-ray analysis.

The solubility of TM in pure ZnSe varies within wide limits. The monophase zinc-blende structure of ZnMeSe can be preserved even up to 35% of Mn, 13% of Fe, and about 2% in the case of Co [30]. The solubilities of Co could reach about 5% and, in the case of V, Cr, and Ni, they do not exceed 1% and are in fact even less than 1% in the case of Ti [31]. Therefore the reflectivity measurements for ternary compounds of ZnSe with V, Cr, Ni, and Ti were limited to just one composition.

The samples were attached to the cold finger of a liquid nitrogen temperature (LNT) cryostat. The reflected beam was collected either with a Bendix M306 electron multiplier in the 10–30 eV energy range or with a solar-blind photomultiplier equipped with a LiF window in the 4–10 eV energy range. Data acquisition was done by means of a lock-in amplifier whose output was digitized and fed into the control computer of the set-up. The reflectivity spectra were reproducible over the entire energy range. Some uncertainty in the fine structure of the broad reflectivity band between 8 and 10 eV was noticed, and this was attributed to the very weak intensity of the detected signal near the cut-off of the grating–detector system.

3. Results and discussion

The analysis of the reflectivity spectra of the ternary compounds $Zn_{1-x}Me_xSe$ (Me = Ti, V, Cr, Mn, Fe, Co, and Ni) was performed from the point of view of the changes in shape and energy position of the characteristic maxima of pure ZnSe. The differences between the spectra of the binary ZnSe and ternary ZnMeSe compounds show the influence of the TM on the electronic band structure of the ZnSe host crystal. The reflectivity spectrum of pure ZnSe, measured and discussed by several research groups [32, 33], is rich in structure. Below, we list the main structures, following the commonly used Cardona notation, and summarize their assignment following the recent work by Markowski *et al* [33]. The reported energies are listed for LNT measurements:

(i) the E_1 (4.88 eV) and $E_1 + \Delta_1$ (5.13 eV) structures arise from transitions between the spin–orbit-split highest valence band and the lowest conduction band along the Λ direction near the L point of the Brillouin zone (BZ), and are well resolved both at RT and LNT;

(ii) the structure corresponding to E_2 arises from a number of critical points of low symmetry in the BZ, and exhibits even more structure at LNT (at 6.40 eV, 6.54 eV, and 6.81 eV);

(iii) the E_0' and $E_0' + \Delta_0'$ (7.24 eV and 7.45 eV) structures correspond to band transitions near Γ and along the Λ and Σ directions, with final states in the second conduction band;

(iv) the E_1' and $E_1' + \Delta_1'$ (8.40 eV and 9.06 eV) structures originate from transitions near the L point, between the highest spin–orbit-split valence band and the second group of conduction bands;

(v) the structures above 11 eV arise mostly from transitions from the Zn 3d and Se 4s core states to the conduction bands;

(vi) the structure at 11.40 eV corresponds to a Zn 3d core exciton at the Γ point, the structure at 11.98 eV being its spin–orbit partner;

(vii) the maxima at 12.20 eV, 12.55 eV, 12.87 eV, and 13.20 eV are assigned to core excitons at the L point, where the degeneracy of the Zn 3d states is completely removed

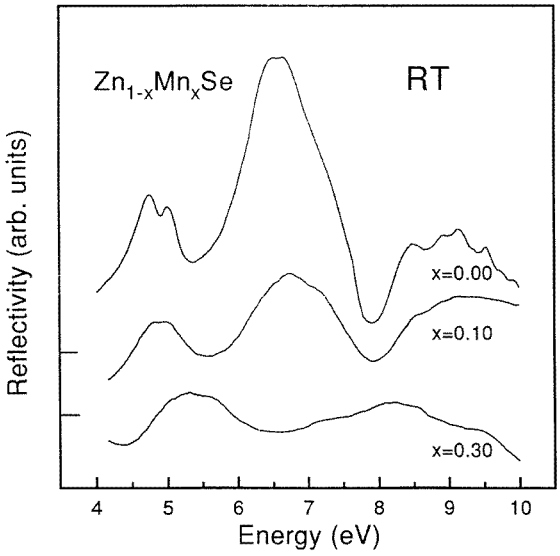

(a)

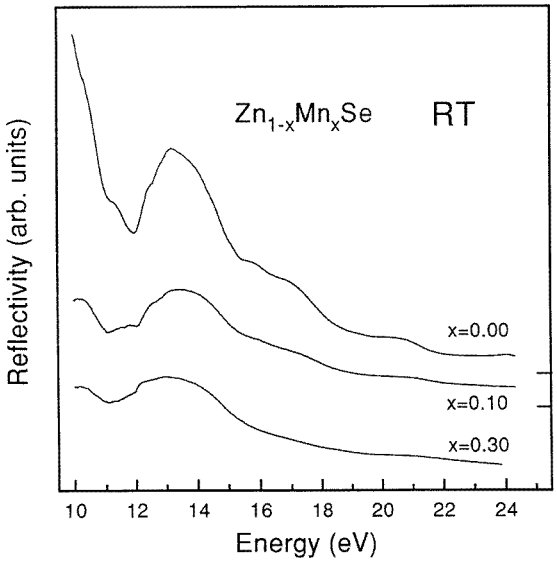

(b)

Figure 1. The reflectivity spectra of $Zn_{1-x}Mn_xSe$ at room temperature (RT): (a) the 4–10 eV energy range; and (b) the 10–25 eV energy range.

(the theory suggests that excitonic transitions at the X point also contribute to the latter two maxima [33]);

(viii) the broad bands with maxima at 15.8 eV, 16.9 eV, 20.5 eV, and 25 eV are attributed to transitions in a large BZ region with initial states in the Zn 3d bands;

(ix) the weaker maxima at about 19 eV and 23 eV are attributed to the contribution from the Se 4s bands.

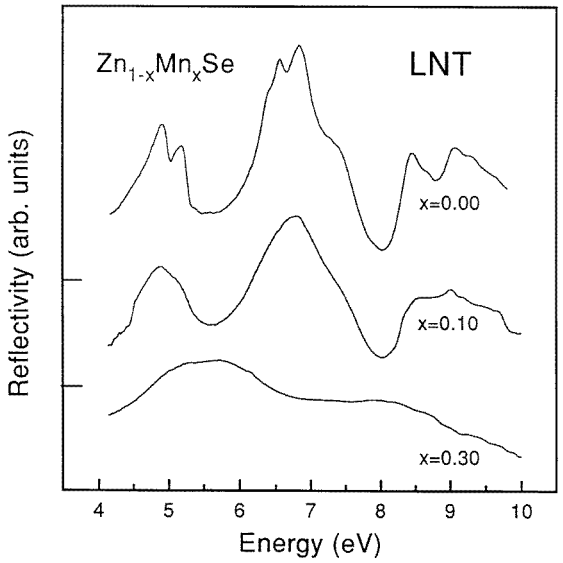

(a)

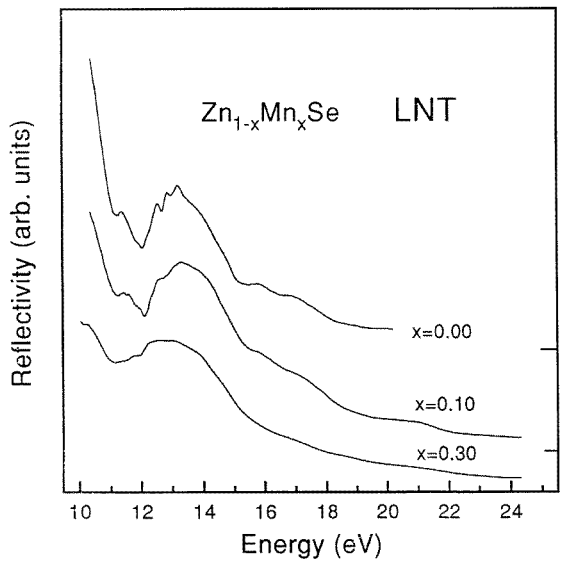

(b)

Figure 2. The reflectivity spectra of $Zn_{1-x}Mn_xSe$ at liquid nitrogen temperature (LNT): (a) the 4–10 eV energy range; and (b) the 10–25 eV energy range.

3.1. $Zn_{1-x}Mn_xSe$

Figures 1 and 2 present the experimental reflectivity spectra for $Zn_{1-x}Mn_xSe$ ($x = 0.10$ and 0.30) for two different energy ranges at room and liquid nitrogen temperatures, respectively. The ZnSe reflectivity spectra are presented for comparison in each figure. The reflectivity spectra measured at LNT have been presented by us in a preliminary report [34], and

are reported here to make the discussion more complete. In the reflectivity spectra of $Zn_{1-x}Mn_xSe$, with increasing Mn content, the two groups of sharp ZnSe structures E_1 and $E_1 + \Delta_1$ as well as E_1' and $E_1' + \Delta_1'$ are almost completely smeared, and shift to higher and lower energies, respectively. The intensity of the E_2-peak decreases rapidly with x, and for the Mn concentration $x = 0.30$ it has completely disappeared both at room and liquid nitrogen temperatures. In the 10–25 eV energy range, the influence of the increasing Mn content is not so strong as in the low-energy range.

In order to discuss the behaviour of the $Zn_{1-x}Mn_xSe$ reflectivity spectra, we completed and applied to ZnMnSe the one-electron model developed for CdMnTe by Taniguchi *et al* [17]. The degenerate Mn 3d atomic states are split by exchange interaction into spin-up and spin-down states. In the high-spin configuration of the Mn atom ($S = 5/2$), the five 3d electrons fully occupy the spin-up states, whereas the spin-down states are not occupied. Both groups of states in the CdTe tetrahedral crystal field are further split into e and t_2 multiplets. Taniguchi *et al* [17] suggested that the e state, for symmetry reasons, does not hybridize with the p-like CdTe states (at the Γ point) responsible for the top of the valence band (VB). The additional maximum at about 3.5 eV binding energy, seen in the electron photoemission of the CdMnTe spectra, has been assigned to the occupied e spin-up states, whereas the t_2 state can hybridize with the VB states of CdTe, and it causes an increase of the global electron photoemission response. The 3d spin-down unoccupied states can interact with the s, p, and d-like CdTe conduction band states.

In bremsstrahlung isochromat spectroscopy (BIS) for CdMnTe, Franciosi *et al* [35] found an additional structure at about 2.0 and 3.5 eV above the conduction band minimum (CBM), attributed to the empty Mn 3d spin-down contribution, and have estimated the exchange splitting between the spin-up and spin-down electrons in CdMnTe as 8.3 eV. In support of these BIS data, Oleszkiewicz *et al* [36] and Kisiel *et al* [37] showed an additional contribution of Mn unoccupied states in the conduction-band- (CB-) projected p-like and s, d-like DOS around the Te atoms, on the basis of XANES data analysis for CdMnTe. The maximum contributions have been estimated to be at 2.0 eV and 3.5 eV above the CBM, respectively.

The energy separation between the additional Mn contribution found in the conduction bands and the e spin-up photoemission structure at 3.5 eV binding energy has been taken by all of these groups as a measure of the exchange splitting of the Mn 3d states in CdMnTe. Therefore, the experimentally estimated value of the spin-up–spin-down exchange splitting in CdMnTe is between 7.2 and 8.7 eV. This value is much larger than those estimated in the LSD calculation of Zunger and co-workers [38, 44] for Mn^{2+} free ions (about 4.5 eV) and by Slater and co-workers [39] for Mn free atoms (about 6 eV).

The above discussion concerning CdMnTe can be directly applied to ZnMnSe ternary compounds. A schematic energy diagram—constructed on the basis of the assumption that the spin-up–spin-down exchange splitting for Mn in CdMnTe and ZnMnSe does not change very much—including the expected bonding and antibonding interactions of the Mn^{2+} states with the ZnSe band structure, is shown in figure 3. Resonant photoemission studies performed for ZnMnSe [10, 11] show a broad peak due to the Mn d states at about 4.0 eV below the VBM (valence band maximum). Assigning this peak to the Mn^{2+} e^2 spin-up states, taking into account the fact that $E_g = 2.8$ eV [2] for $Zn_{0.9}Mn_{0.1}Se$ and an experimental exchange splitting of 8.3 eV [35], as was estimated in the case of CdMnTe, we can expect for ZnMnSe the maximum contribution of the unoccupied 3d states of Mn^{2+} at about 1.5 eV above the CBM. A similar result has been obtained by Weidemann *et al* [10], who estimated the exchange splitting for ZnMnSe to be equal to 7.6 eV. The analysis of the XANES spectra of ZnMnSe also supports this estimation [40]. It shows that Mn s

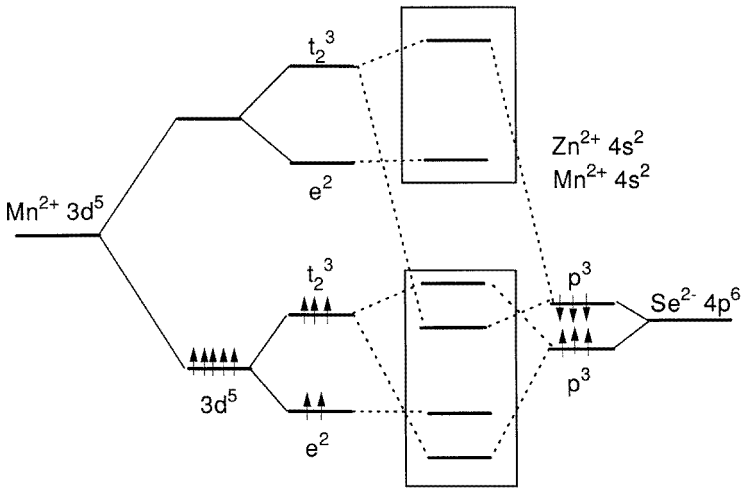

Figure 3. A schematic energy diagram of the s, p–d coupling for ZnMnSe.

and d hybridized states contribute predominantly to the p-like DOS of ZnMnSe very close to the CBM.

According to the above analysis and the ZnMnSe energy diagram presented in figure 3, the Mn^{2+} 3d states have a substantial influence on the whole VB structure and on the lowest CB at Γ_6^c–L_6^c–X_6^c and the second lowest CB at the X point (X_7^c). The influence of Mn^{2+} states on the higher CBs should be weaker. Therefore, because E_1, $E_1 + \Delta_1$, and E_1', $E_1' + \Delta_1'$ are transitions from the highest spin–orbit-split VB in the Λ direction, nearly at the L point, to Λ_6^c and Λ_6^c, $\Lambda_{4,5}^c$ at the first and second conduction band critical points of the BZ, a steady smearing of those structures with increase of the Mn content is related to a strong interaction of the Mn^{2+}-ion states with the band structure of the ZnSe matrix. Also, the optical transitions in the 10–25 eV energy range from the Zn $4d^{10}$ core states to the lowest conduction bands at the L, Γ, X points, which are strongly modified by the influence of the Mn^{2+} states, show a strong sensitivity to the increase of Mn concentration. For the Mn concentration $x = 0.30$, the maximum E_2 completely disappears both at room and liquid nitrogen temperatures. This implies a severe local distortion of the crystal lattice, which could be associated with a strong local stress. The E_2-maximum derives from transitions occurring at a large number of low-symmetry critical points in the volume of the BZ, which are well known to be affected by stress [41] and topological disorder, which can cause the decrease of the symmetry of the crystal and therefore have a substantial influence on the optical transitions, mainly at low-symmetry critical points in the BZ.

3.2. $Zn_{1-x}Fe_xSe$

Figures 4 and 5 present the fundamental reflectivity spectra of $Zn_{1-x}Fe_xSe$ ($x = 0.01$, 0.05, and 0.10) measured at RT and LNT in the 4–10 eV and 10–25 eV energy ranges, respectively. The LNT experimental data have also been reported in a preliminary form elsewhere [34]. A general analysis of the ZnFeSe reflectivity spectra shows large similarities between their shape and that of the spectrum of the host crystal. The observed structures are fairly smeared, and some of them (E_1 and $E_1 + \Delta_1$) are slightly shifted towards higher energies at both temperatures. The spectra at RT are smeared to a much greater degree than

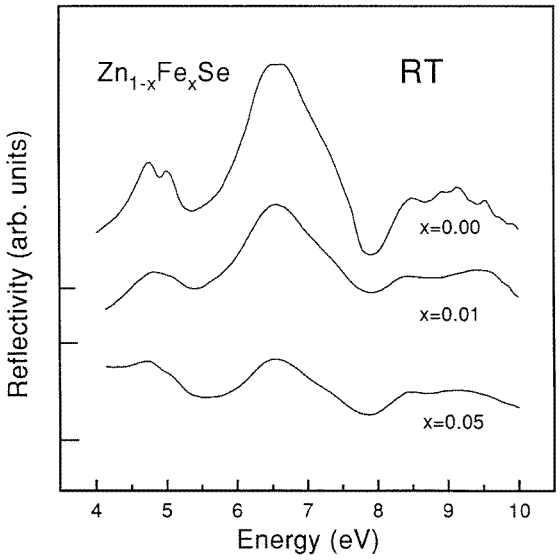

(a)

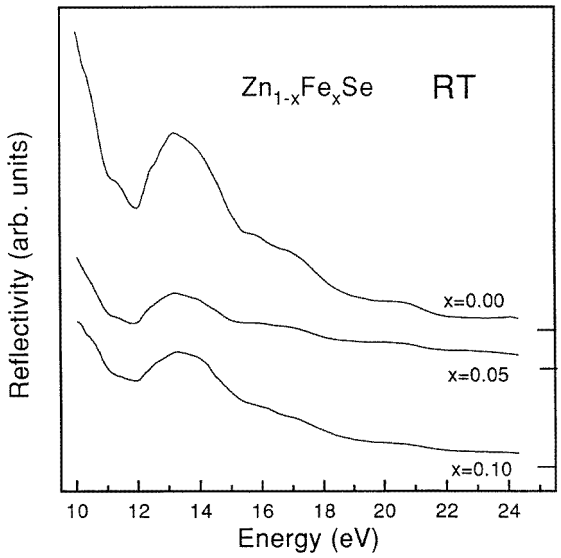

(b)

Figure 4. The reflectivity spectra of $Zn_{1-x}Fe_xSe$ at room temperature (RT): (a) the 4–10 eV energy range; and (b) the 10–25 eV energy range.

the LNT ones. A similar behaviour is observed also for the structures E_1' and $E_1' + \Delta_1'$. The E_2-maximum loses its fine structure, but its energy position remains unchanged. In the 10–25 eV energy range, the broad band with a maximum at about 13.5 eV is shifted to higher energies while the iron content increases, as was already noticed for the ternary compounds containing manganese.

The differences observed in the ZnFeSe reflectivity spectra can be explained by

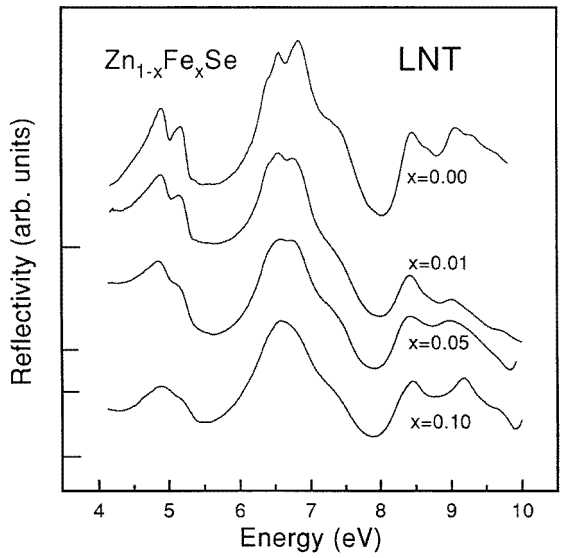

(a)

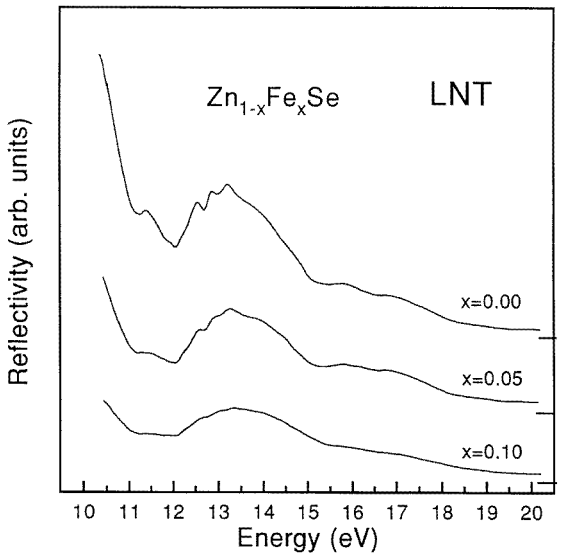

(b)

Figure 5. The reflectivity spectra of $Zn_{1-x}Fe_xSe$ at liquid nitrogen temperature (LNT): (a) the 4–10 eV energy range; and (b) the 10–25 eV energy range.

considering the influence of Fe-ion states on the band structure of the ZnSe host crystal. As the necessary basis for the analysis of the ZnFeSe reflectivity spectra, we have applied the models proposed at first for CdFeSe by Kisiel *et al* [19], and subsequently developed by Sarem *et al* [21] and Taniguchi *et al* [22]. Like the Mn^{2+} 3d states, the Fe^{2+} 3d states are first split by the exchange interaction into spin-up and spin-down states. Each of these states is further split by the tetrahedral crystal field into e and t_2 states. In the Fe^{2+} high-

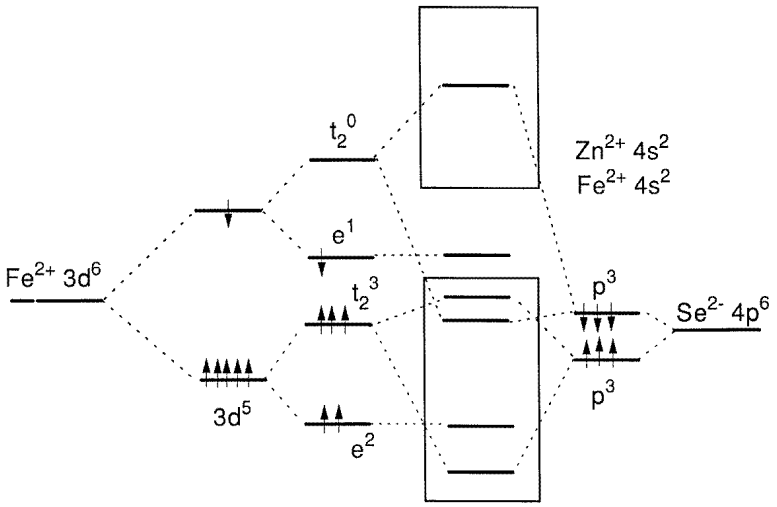

Figure 6. A schematic energy diagram of the s, p–d coupling for ZnFeSe.

spin configuration ($S = 2$), the five spin-up electrons fill a non-hybridizing doublet of e symmetry, and the t_2 triplet hybridizes with p-like VB wave functions at the Γ point. The sixth Fe 3d electron half fills the spin-down e state, that should be localized inside the forbidden gap as a deep donor, like the Fe^{2+} contribution in CdFeSe [19–21, 42]. The t_2 spin-down unoccupied states should hybridize with the conduction bands.

Using a more sophisticated mean-field approximation, the multielectron ground-state term ^5E of the Fe^{2+} ($e^3t_2^3$) electron configuration creates a deep donor state inside the forbidden gap of ZnFeSe [43, 44], which is consistent with the less precise, but more pictorial schematic one-electron energy diagram proposed in figure 6. In this energy diagram, bonding and antibonding interactions between the Fe d states and the band structure of the ZnSe host crystal have been considered. Resonant photoemission measurements performed on ZnFeSe show two Fe-related structures at 3.4 eV and 0.9 eV below the VBM and a third structure at about 0.2 eV above the ZnSe VBM [11]. The last feature could be identified as a deep donor state situated inside the forbidden energy gap. The energy position of this feature is in general agreement with the analysis of photoacoustic measurements, in which the Fe^{2+} ground state has been located at 0.6 eV above the VBM [26]. Poor agreement is found with the position of the deep donor state, reported by Zunger [44] after Dieleman *et al* [45], at about 1.1–1.3 eV above the VBM. Whereas in both photoemission and photoacoustic spectroscopy one electron is removed from the Fe^{2+} $3d^6$ ground state and transferred to the ZnSe CB, the value reported by Dieleman *et al* [45] corresponds to the photon energy required to excite an electron from the VB to the Fe^{3+} (d^5) state. The charge states of the Fe ion are different in the two cases, and the ionization values are not comparable, since the relaxation energy should be considered (see p 352 of [44] and references therein). The energy position of the 3.4 eV maximum reported by Lama *et al* [11], which is related to non-hybridizing e-symmetry spin-up electrons, is in very good agreement with photoemission results obtained for CdFeSe [22, 46].

The energy positions of the non-hybridized e^2 spin-up states for Fe^{2+} are also almost equal to values obtained for Mn^{2+} in zinc sulphides, selenides, and tellurides [10, 11, 47]. This behaviour of the e^2 states of Mn^{2+} and Fe^{2+} is also confirmed by calculations [44, 48].

Table 1. The basic properties of the transition metal ions in zinc-blende ZnMeSe ternary compounds. The average energy of the deep-donor position is referred to the top of the VBM of ZnSe. The column headings on the right-hand side have the following meanings: (a) the values given by Slater *et al* [39], which have been calculated for free atoms; (b) the values given by Zunger [44], which have been calculated, for free ions, using the LSD method; (c) the values given by Hołda *et al* [48], which have been calculated for $Zn_{0.5}Me_{0.5}Se$ compounds using the LMTO method; (d) the values taken from table VII in [44]; (e) the values given by Felici *et al* [26]; (f) the values given by Langer and Heinrich [43]; (g) the energy position of the e^2 spin-up electrons (below the VBM): (α) the values given by [10, 11]; (β) the values given by [11]; and (γ) the values given by Langer and Heinrich [43].

Element Me	Electronic configuration	Spin configuration	Ground state	Exchange splitting (eV)			Deep-donor position (eV)			
				(a)	(b)	(c)	(d)	(e)	(f)	(g)
Ti^{2+}	e^2	1	$^3A_2$	1.8		0.06	1.75		1.76	
V^{2+}	$e^2t_2^1$	3/2	$^4T_1$	2.97	2.4	1.96	Gap		1.73	
Cr^{2+}	$e^2t_2^2$	2	$^5T_2$	4.91	3.4	3.27	0.46		0.70	
Mn^{2+}	$e^2t_2^3$	5/2	$^6A_1$	5.8	4.5	3.96	VB			3.8–4.0 (α)
Fe^{2+}	$e^3t_2^3$	2	^5E	4.95	3.6	2.96	1.1–1.3	0.6	0.89	3.5 (β)
Co^{2+}	$e^4t_2^3$	3/2	$^4A_2$	3.95	2.8	1.94	0.3	0.5	0.37	3.4 (γ)
Ni^{2+}	$e^4t_2^4$	1	$^3T_1$	2.78	1.95	0.76	0.5	1.1	0.36	

The Fe^{2+} unoccupied states, which hybridize with the CB of host crystal, can be seen in XANES spectra of the Se K edge [40], as a p-like contribution at about 1.7 eV below the CBM of pure ZnSe. Because the chemical shift of the Se K edge for ZnFeSe is less than 1 eV, the contribution of the Fe d states lies about 1 eV below the ZnFeSe CBM. The theoretical LMTO calculations of the p-like DOS contribution of the Fe d states in $Zn_{0.5}Fe_{0.5}Se$ indicate p-like states localized at about 0.6 eV above the Fermi level [49]. Together with known experimental and theoretical evidence, this information is shown in figure 6. According to the above analysis, it is easy to ascertain that the t_2 spin-up electrons of Fe^{2+} interact strongly with the upper part of the VB of the ZnSe host crystal. Creation by the sixth spin-down electron of the deep donor state in the forbidden energy gap and the ∼25% smaller spin-up–spin-down interaction splitting in Fe^{2+} [40, 44, 48, 49] (see also table 1) makes the influence of unoccupied Fe states on the CBs weaker. This can be seen on comparing ZnMnSe and ZnFeSe reflectivity spectra (10% Mn and Fe compositions). The influence of Fe^{2+} seems to be smaller around the $L^c_{4,5}$ second CB than it is in the case of Mn^{2+}, because the structures E_1' and $E_1' + \Delta_1'$ are less blurred for 10% Fe content than for 10% Mn content. Because the spin-up and spin-down splitting in Fe^{2+} free ions is about 25% lower than for Mn^{2+}, the contribution of the hybridized states of Fe^{2+} should be more significant in the lowest part of the CB. In the case of the maxima E_1 and $E_1 + \Delta_1$, which are assigned to the transitions from the VB to the lowest CB in the Λ direction, as well as in the case of core transitions from Zn 4d and Se 4s to the lowest CB, the smearing of the structures discussed caused by Fe is comparable with that caused by the presence of Mn in the ZnSe host crystal.

In general, the one-electron approximation cannot represent a complicated picture of a many-electron interaction system. An analysis of the mean-field approach presented by Zunger [44], as has been mentioned above, leads to results for ZnMnSe and ZnFeSe which were confirmed by experiment. For the other TMs, i.e. Co, Ni, Cr, V, and Ti, the general

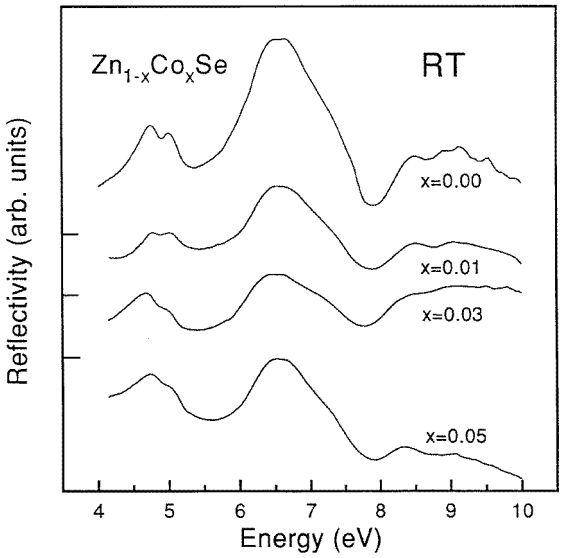

(a)

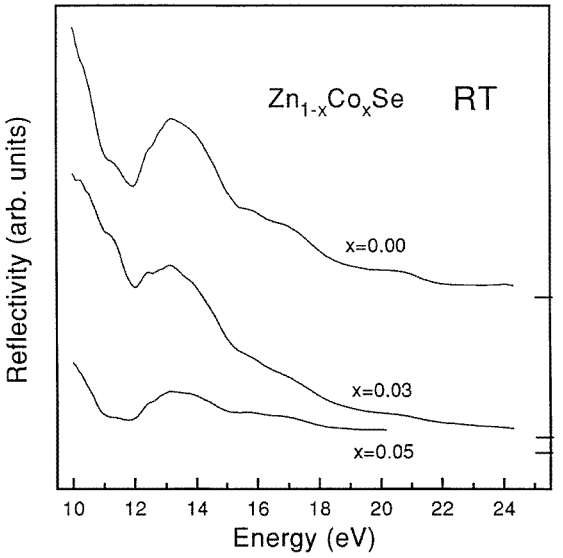

(b)

Figure 7. The reflectivity spectra of $Zn_{1-x}Co_xSe$ at room temperature (RT): (a) the 4–10 eV energy range; and (b) the 10–25 eV energy range.

features of the energy diagram presented for ZnFeSe (figure 6), which presents the tendencies of the hybridization of occupied and unoccupied d states of TM, can be adapted to each TM, according to the number of electrons in the 3d sub-shell and to the decrease of the spin-up–spin-down exchange splitting. Therefore, in the model analysis of the contribution of the 3d TM to the band structure of ZnMeSe ternary compounds, several important distinctive features should be taken into consideration:

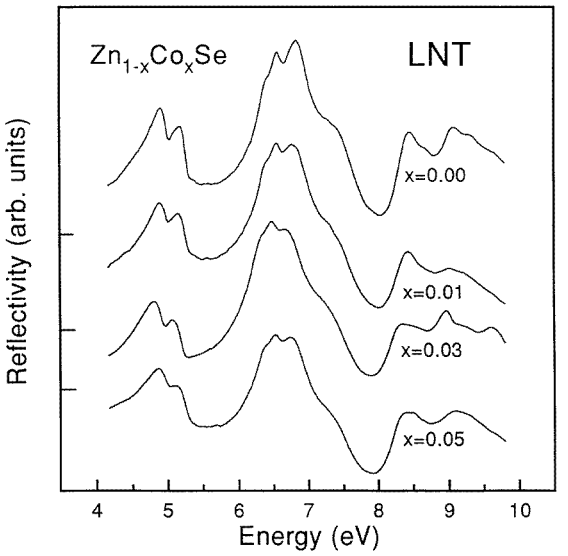

(a)

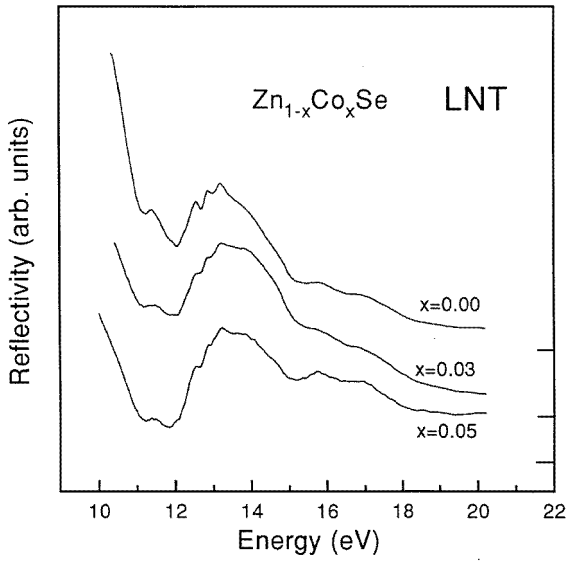

(b)

Figure 8. The reflectivity spectra of $Zn_{1-x}Co_xSe$ at liquid nitrogen temperature (LNT): (a) the 4–10 eV energy range; and (b) the 10–25 eV energy range.

(1) the ground state for each $3d^n$ configuration should be defined in terms of many-electron configurations [44];

(2) in the case of ZnMeSe ternary compounds, the ground state is, with the exclusion of the case for Mn, situated inside the forbidden gap of ZnSe, and is identified as a deep donor state; the experimental energy positions of the deep donor levels with respect to the VBM are listed in table 1;

(3) the spin-up–spin-down exchange splitting of the 3d states is at its maximum for the Mn^{2+} ion, and decreases monotonically for the other TMs in the sequences Mn, Fe, Co, Ni, and Mn, Cr, V, Ti [44, 48].

On the basis of the above remarks and the estimated spin-up–spin-down electron exchange splitting listed in table 1, as well as at the energy positions of deep donors created by TMs in ZnSe host crystal, we can deduce the influence of the 3d states of TMs on the fundamental reflectivity spectra.

3.3. $Zn_{1-x}Co_xSe$

The reflectivity spectra of ZnCoSe, shown in figures 7 and 8, were measured in the 4–10 eV and 10–25 eV energy ranges at LNT and RT, respectively. The experimental data have been reported in a preliminary form elsewhere [4]. The spectra taken at RT are less structured in comparison with LNT spectra, showing the normal behaviour of semiconducting compounds. Generally, the presence of Co ions in $Zn_{1-x}Co_xSe$ (nominal content $x = 0.01$, 0.03, and 0.05) leads to some changes in the relative intensities of the reflectivity structures as well as to some shifts of the energy positions of the observed maxima, but these changes are quite small in comparison with those caused by the presence of Mn or Fe. In addition, the influence of the presence of Co is much more visible in the low-energy range than in the high-energy region, where the transitions from core levels to conduction bands occur. At both RT and LNT the maxima E_1 and $E_1 + \Delta_1$ become less pronounced, smeared, and slightly shifted towards higher energies with increase of the Co content. The E_2-maximum, split at LNT, does not seem to move in energy when Co ions replace Zn ones in the cation sublattice. The E_0'-shoulder is clearly visible even for the highest concentration, whereas the structures E_1' and $E_1' + \Delta_1'$ are blurred.

In the tetrahedral crystal field, Co^{2+} ions in high-spin configurations ($S = 3/2$) have $e^4t_2^3$ electron configurations. The multiplet ground-state term $^4A_2$ is localized inside the ZnCoSe forbidden gap as a deep donor state lying very close to the VBM. In fact, Nores *et al* [50] and Felici *et al* [26] localized it at 0.62 eV and 0.5 eV, respectively, but according to Zunger [44] this donor state is situated at 0.3 eV above the VBM.

From the values reported in table 1, it is evident that the exchange splitting for Co^{2+} ions is much smaller than in the case of Mn^{2+} and Fe^{2+} ions. Therefore, the contribution of Co^{2+} occupied states to the VB should be significant, but the hybridization of unoccupied Co^{2+} 3d states with the CB should be weaker. XANES analysis and LMTO calculations [49] suggest that the contribution of the Co 3d empty states to the p-like CB DOS is situated close to the CBM, i.e. about 0.5 eV below the CBM of the host crystal and 0.37 eV above the Fermi energy, respectively.

The energy positions of the reflectivity structures above 10 eV do not change significantly on increasing the Co concentration, but their relative intensities decrease, which is evidently correlated with the increase of topological disorder. It could be also caused by small changes in the conduction band state distribution associated with the presence of Co states, in support of the statement made above concerning the much weaker influence of Co^{2+} unoccupied states in the CB region on the band structure of the ZnSe host crystal.

3.4. $Zn_{1-x}Ni_xSe$

The reflectivity spectrum of $Zn_{0.99}Ni_{0.01}Se$, taken at LNT in the 4–10 eV energy range, is shown in figure 9. The main shape remains the same as for pure ZnSe; however, the energy positions of all of the maxima, characteristic for pure ZnSe, are shifted to lower energies.

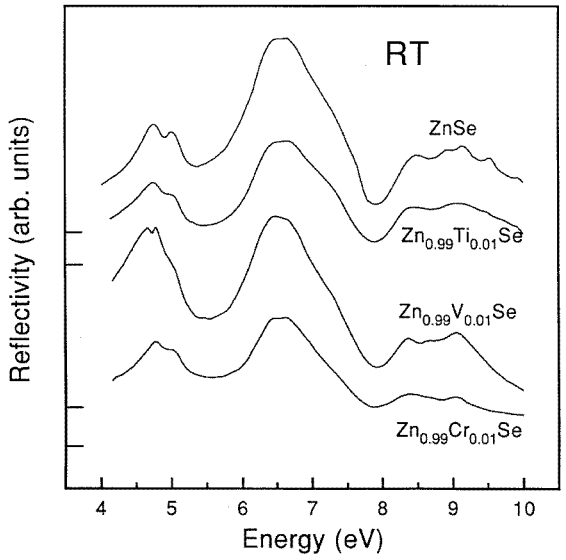

(a)

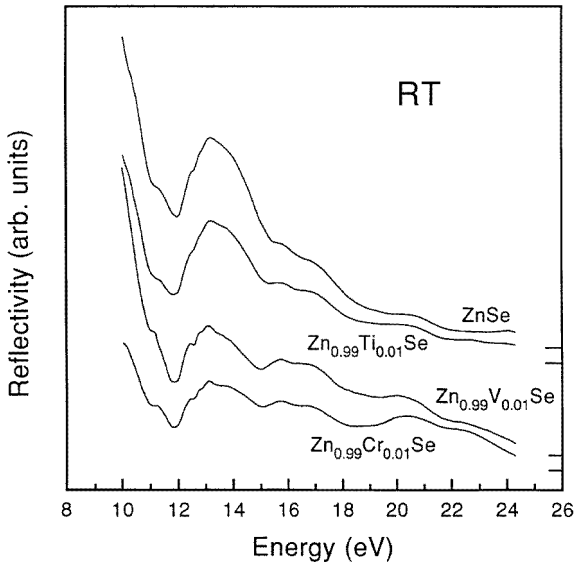

(b)

Figure 9. The reflectivity spectra for $Zn_{1-x}Cr_xSe$, $Zn_{1-x}V_xSe$, and $Zn_{1-x}Ti_xSe$ at room temperature (RT): (a) the 4–10 eV energy range; and (b) the 10–25 eV energy range.

The E_2-maximum does not lose its fine structure, but its intensity is relatively lower. As was expected, the reflectivity structures are slightly blurred. On the basis of this behaviour we can suggest that Ni ions cause some changes in the valence bands of pure ZnSe near and at the L point in the BZ, and that the influence of the Ni 3d empty states on the CBs should be smaller. This suggestion is understandable on the basis of the model developed for ZnFeSe (figure 6) and ZnCoSe using experimental and theoretical data concerning the

spin-up and spin-down electron energy positions and their exchange splitting. The mean energy position of five spin-up electrons, which are immersed and partially hybridized in the valence band of the ZnSe host crystal, is situated about 3.5 eV below the VBM [9]. Hołda *et al* [51], on the basis of LMTO calculations, have estimated a mean value for the spin-up electron energy position of 1.51 eV below the Fermi level. The multielectron $^3T_1$ ground state of the Ni $3d^8$ electrons is situated 0.5 above the VBM as a deep donor [44] (see table 1). The spin-up–spin-down exchange splitting calculated using the LDA method is 1.95 eV, and that calculated using the LMTO method is 0.76 eV [48]. These data suggest a significant influence of spin-up electrons on the VB of the ZnSe host crystal, and a rather small contribution of Ni unoccupied 3d states to the conduction bands of ZnSe.

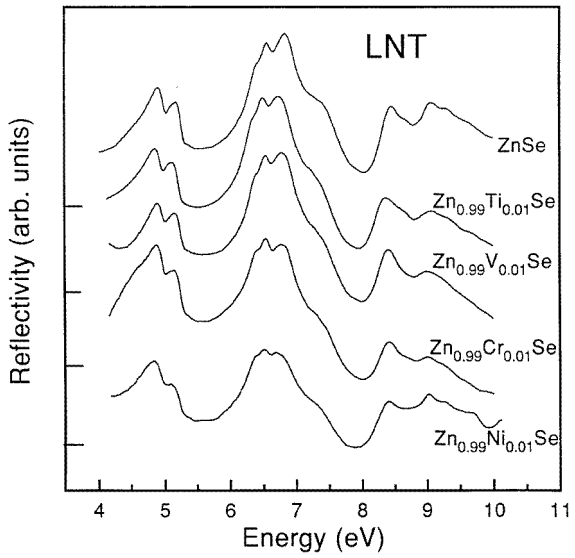

Figure 10. The reflectivity spectra of $Zn_{1-x}Ni_xSe$, $Zn_{1-x}Cr_xSe$, $Zn_{1-x}V_xSe$, and $Zn_{1-x}Ti_xSe$ at liquid nitrogen temperature in the 4–10 eV energy range.

3.5. $Zn_{1-x}Cr_xSe$

The fundamental reflectivity measurements of $Zn_{1-x}Cr_xSe$ ($x = 0.01$) were performed in the 4–10 eV and 10–25 eV energy ranges at RT and LNT, respectively (see figures 9 and 10). Apart from the expected blurring found at both temperatures, very small differences between the reflectivity spectra of the ternary compound and the host crystal are noticed. The energy positions of the maxima are the same as for pure ZnSe over the entire energy range, other than those of the group of the structures E_1' and $E_1' + \Delta_1'$, which shift to lower energies.

In the tetrahedral crystal field, Cr^{2+} ions in the high-spin configuration ($S = 2$) have the $e^2t_2^2$ electron configuration. The multiplet ground-state term $^5T_2$ is localized inside the ZnCrSe forbidden gap at 0.46 eV above the VBM [44] as a deep donor. The energy position of the the Cr^{2+} deep donor state and the exchange splitting energy are close to the respective values for Fe^{2+} [44, 48]. Therefore, the contribution of the occupied Cr^{2+} $3d^4$ spin-up electron states and $3d^6$ unoccupied states should affect the valence and conduction bands of the host ZnSe crystal in a similar way to what is seen for ZnFeSe. This behaviour

can be observed on comparing the ZnCrSe and ZnFeSe reflectivity spectra. These spectra present similar tendencies, i.e. smearing of the spectrum in the 4–10 eV energy region, particularly the maxima E_1' and $E_1' + \Delta_1'$, and in the 10–25 eV range, where transitions from Zn $3d^{10}$ states to the first CB are observed. Therefore, one can assume a significant contribution of Cr-ion states in the upper part of the conduction bands, particularly at the $L_{4,5}^c$ point of the BZ, which causes the observed smearing of the reflectivity spectrum.

3.6. $Zn_{1-x}V_xSe$

In the tetrahedral crystal field the V^{2+} ions in the high-spin configuration ($S = 3/2$) have the $e^2t_2^1$ electron configuration. As has been reported by Zunger [44], the ground state $^4T_1$ is localized in the ZnSe forbidden energy gap as a deep donor. Unfortunately, the energy position of this deep donor is not directly known, but it can be estimated as 1.73 eV above the VBM from the paper by Langer and Heinrich [43] and recently obtained electron paramagnetic resonance results for CdTe:V [52]. The mean energy position of the occupied and empty spin-up electron states is about 0.2 eV below E_F [48]; therefore a limited influence of the spin-up occupied states on the valence band of ZnSe should be expected. A spin-up–spin-down exchange splitting of 1.96 eV has been estimated by Markowski *et al* [53] for $Zn_{0.5}V_{0.5}Se$; therefore the influence of V^{2+} ions on the conduction band structure should be higher than that for the valence band.

Figures 9 and 10 show ZnVSe reflectivity spectra in comparison with reflectivity spectra for pure ZnSe and other ternary compounds composed of a transition metal and ZnSe. This comparison supports the above suggestion. In the ZnVSe reflectivity spectrum, in the 10–25 eV energy range (figure 10), the fine structures observed for pure ZnSe crystal are preserved, but only the relative intensities for ZnVSe are lower. This suggests a poorer quality of the ZnVSe sample in comparison with the ZnSe. In the fundamental reflectivity spectrum in the energy range 4–10 eV, the structures E_1 and $E_1 + \Delta_1$ partially disappear at RT (figure 9(a)), while at LNT (figure 10) they show rather slight blurring.

3.7. $Zn_{1-x}Ti_xSe$

In the tetrahedral crystal field the Ti^{2+} ions in the high-spin configuration ($S = 1$) have the e^2 electron configuration, which creates a multiplet ground state $^3A_2$ localized in the ZnSe forbidden energy gap as a deep donor at about 1.75 eV above the VBM [44]. In the e^2 electron configuration, for symmetry reasons, both spin-up electrons cannot interact with the VB p states; therefore we expect very weak hybridization of the Ti 3d occupied states with the valence band states. The spin-up–spin-down exchange splitting, as has been reported by Slater *et al* [39] for Ti atoms, equals 1.8 eV, but according to LMTO calculations for $Zn_{0.5}Ti_{0.5}Se$ made by Hołda *et al* [48], this splitting is extremely small and is equal to 0.06 eV. Thus the influence of the spin-up and spin-down empty states on the conduction bands should be very small.

The reflectivity spectra of $Zn_{1-x}Ti_xSe$ (for x less than 0.01) were taken at RT and LNT in the 4–10 eV (figures 9(a) and 10(a)) and 10–25 eV (figures 9(b) and 10(b)) energy ranges. The analysis of the reflectivity structures shows very slight changes in energy positions of the main maxima. The shapes of both the RT and the LNT spectra remain almost unchanged. The only observed differences appear in the low-energy range at both temperatures. The group of maxima E_1' and $E_1' + \Delta_1'$ shift slightly towards lower energy while the energy positions of the peaks E_1 and $E_1 + \Delta_1$ remain the same. The intensity of the E_2-maximum decreases in comparison with that for pure ZnSe, but its fine structure

is preserved. Moreover, the E_0'-shoulder is very clearly pronounced. The observed small changes of the reflectivity spectra suggest that the influence of Ti^{2+} ions appears more strongly in the conduction bands of the ZnSe host crystal.

4. Conclusions

In this paper, the fundamental reflectivity spectra for ZnMeSe solid solutions with several transition metals (Ti, V, Cr, Mn, Fe, Co, and Ni) have been presented. The influence of the $3d^n$ subshell of the transition metals on the valence and conduction bands of the ZnSe host crystal was discussed. Using known experimental and theoretical data and taking into account the data collected together in table 1, we have suggested consistent models of the influence of various transition metals on the valence and conduction bands of ZnSe which can explain the behaviour of the fundamental reflectivity spectra of ZnMeSe solid solutions with the transition metals. It has been shown that a significant influence on the fundamental reflectivity spectra is observed for almost all TMs, and this influence decreases in the sequences Mn, Fe, Co, and Ni as well as Mn, Cr, V, and Ti. This influence is the smallest for Ni and Ti particularly, because of very small exchange splitting for Ti (see table 1). The contribution of Ti 3d states to the valence and conduction bands of ZnSe host crystal seems to be rather small.

Acknowledgments

This work was partially supported by the Direct Research Exchange Programme of the Universitá degli Studi di Roma 'La Sapienza' and the Jagellonian University, and by the National Polish Committee of Research, contracts C/2733/95, C/3659/96, and C/039/97, as well as by the INFM (Istituto Nazionale di Fisica della Materia). One of us (DD) is grateful for financial support to the Italian Ministero degli Affari d'Esteri.

References

[1] Furdyna J K 1982 *J. Appl. Phys.* **53** 7637
Ramdas A K 1982 *J. Appl. Phys.* **53** 7649
[2] Furdyna J K and Kossut J 1988 *Semiconductors and Semimetals* vol 25, ed R K Willardson and A C Beer (San Diego, CA: Academic)
[3] Mak C-L, Sooryakumar R, Steiner M M and Jonker B T 1993 *Phys. Rev.* B **48** 11 743
[4] Dębowska D, Zimnal-Starnawska M, Kisiel A, Piacentini M, Zema N, Lama F and Giriat W 1995 *Acta Phys. Pol.* A **87** 275
[5] Martinez L, Gonzalez L R and Giriat W 1993 *Phys. Status Solidi* b **180** 267
[6] Roa L, Vincent A B and Joshi N V 1992 *J. Phys. Chem. Solids* **53** 261
[7] Goetz G, Pohl U W and Schulz H J 1992 *J. Phys.: Condens. Matter* **4** 8253
[8] Joshi N V, Matta M, Quitero P and Martin J M 1991 *Solid State Commun.* **80** 43
[9] Kim J D, Cooper S L, Klein M V and Jonker B T 1994 *Phys. Rev.* B **49** 1732
[10] Weidemann R, Gumlich H-E, Kupsch M, Middelmann H-U and Becker U 1992 *Phys. Rev.* B **45** 1172
[11] Zema N, Lama F, Piacentini M, Felici A C, Dębowska D, Kisiel A and Olson C G 1995 *Acta Phys. Pol.* A **87** 495
Dębowska D, Zema N, Piacentini M, Lama F, Felici A C, Kisiel A and Olson C G 1994 *Properties of f-electron Compounds* ed A Szytula (Cracow: Jagellonian University Press) p 9
Lama F, Zema N, Felici A C, Piacentini M, Dębowska D and Kisiel A 1997 to be published
[12] Twardowski A, Fries T, Shapira Y, Eggenkamp P, Swagten H J M and Demianiuk M 1993 *J. Appl. Phys.* **73** 5745
Karthauser E, Rodriguez S and Villert M 1993 *Phys. Rev.* B **48** 14 127

[13] Zimnal-Starnawska M, Podgorny M, Kisiel A, Giriat W, Demianiuk M and Žmija J 1984 *J. Phys. C: Solid State Phys.* **17** 615
[14] Lautenschlager P, Logothetidis S, Viña L and Cardona M 1985 *Phys. Rev.* B **32** 3811
[15] Kendelewicz J 1980 *Solid State Commun.* **36** 127
[16] Kisiel A, Piacentini M, Antonangeli F, Oleszkiewicz J, Rodzik A, Zema N and Mycielski A 1987 *J. Phys. C: Solid State Phys.* **20** 5601
[17] Taniguchi M, Ley L, Johnson R L, Gijsen J and Cardona M 1986 *Phys. Rev.* B **33** 1206
[18] Dębowska D, Zimnal-Starnawska M, Rodzik A, Kisiel A, Piacentini M, Zema N and Giriat W 1993 *J. Phys.: Condens. Matter* **5** 9345
[19] Kisiel A, Piacentini M, Antonangeli F, Zema N and Mycielski A 1989 *Solid State Commun.* **70** 693
[20] Piacentini M, Dębowska D, Kisiel A, Markowski R, Mycielski A and Zema N 1993 *J. Phys.: Condens. Matter* **5** 3707
[21] Sarem A, Kowalski B J and Orłowski B A 1990 *J. Phys.: Condens. Matter* **2** 8173
[22] Taniguchi M, Ved Y, Morisada I, Murashita Y, Ohta T, Sonma I and Oka Y 1990 *Phys. Rev.* B **41** 3069
[23] Furdyna J K 1988 *J. Appl. Phys.* **64** R29
Mycielski A 1988 *J. Appl. Phys.* **63** 3279
[24] Castillo M 1992 *Int. J. Infrared Millimeter Waves* **13** 909
[25] Hwang I, Lee J Y, Kim J-E and Park H Y 1992 *Phys. Status Solidi* b **173** K29
[26] Felici A C, Lama F, Piacentini M, Papa T, Dębowska D, Kisiel A and Rodzik A 1996 *J. Appl. Phys.* **80** 6925
[27] Mac W, Khoi N T, Twardowski A, Gaj J A and Demianiuk M 1993 *Phys. Rev. Lett.* **71** 2327
Mac W, Twardowski A, Eggenkamp P J T, Swagten H J M, Shapira Y and Demianiuk M 1994 *Phys. Rev.* B **50** 14 144
[28] Bhattacharjee A K 1994 *Phys. Rev.* B **49** 13 987
[29] Rabago F, Vincent A B and Joshi N V 1990 *Mater. Lett.* **9** 480
[30] Hwang I, Kim H, Kim J-E, Park H Y and Lim H 1994 *Phys. Rev.* B **50** 8849
[31] Giriat W 1996 private communication
[32] Cardona M 1961 *J. Appl. Phys.* **32** 2151
Ebina A, Yamamoto M and Takahashi T 1972 *Phys. Rev.* B **6** 3786
Petroff Y, Balkanski M, Walter J P and Cohen M L 1969 *Solid State Commun.* **7** 459
Walter J P, Cohen M L, Balkanski M and Petroff Y 1970 *Phys. Rev.* B **1** 2661
Freeouf J L 1973 *Phys. Rev.* B **7** 3810
[33] Markowski R, Piacentini M, Dębowska D, Zimnal-Starnawska M, Lama F, Zema N and Kisiel A 1994 *J. Phys.: Condens. Matter* **6** 3207
[34] Zimnal-Starnawska M, Dębowska D, Kisiel A, Piacentini M, Lama F, Zema N and Giriat W 1994 *Acta Phys. Pol.* A **86** 869
[35] Franciosi A, Wall A, Gao Y, Weaver J H, Tsai M H, Dow J D, Kasowski R V, Reifenberger R and Pool F 1989 *Phys. Rev.* B **40** 12 009
[36] Oleszkiewicz J, Podgorny M, Kisiel A, Dalba G, Rocca F and Burattini E 1990 *Proc. 2nd European Conf. on Progress in X-ray Synchrotron Radiation Research* vol 25, ed A Balerua, E Bernieri and S Mobilio (Bologna: SIF)
[37] Kisiel A, Ali Dahr A-I, Lee P M, Dalba G, Fornasini P and Burattini E 1991 *Phys. Rev.* B **44** 11 075
[38] Wei S-H and Zunger A 1987 *Phys. Rev.* B **35** 2340
[39] Slater J C, Mann J B, Wilson T M and Wood J H 1969 *Phys. Rev.* **184** 672
[40] Lee P M, Kisiel A, Burattini E and Demianiuk M 1994 *J. Phys.: Condens. Matter* **6** 5771
[41] Kisiel A, Pukowska B and Ignatowicz S A 1980 *Thin Solid Films* **67** 57
[42] Mycielski A, Dzwonkowski P, Orłowski B, Dobrowolska M, Arciszewski H, Dobrowolski W and Baranowski J M 1986 *J. Physique* **19** 3605
[43] Langer J M and Heinrich H 1985 *Phys. Rev. Lett.* **55** 1414
[44] Zunger A 1986 *Solid State Physics* vol 39 (New York: Academic) p 275
Fazzio A, Caldas M J and Zunger A 1984 *Phys. Rev.* B **30** 3430
[45] Dieleman J, de Jong J W and Meijer T 1966 *J. Chem. Phys.* **45** 3178
[46] Denecke R, Ley L and Fraxedas J 1993 *Phys. Rev.* B **47** 13 197
[47] Mimura K, Happo N, Sato H, Harada J, Miyazaki K, Namatame H, Taniguchi M, Ohashi M and Ueda Y 1996 *J. Electron Spectrosc. Relat. Phenom.* **79** 12
[48] Hołda A, Markowski R, Dębowska D, Kisiel A, Zema N, Lama F, Zimnal-Starnawska M and Piacentini M 1997 to be published
[49] Kisiel A, Lee P M, Burattini E and Giriat W 1997 to be published

[50] Nores J M, Szawelska M R and Allen J W 1981 *J. Phys. C: Solid State Phys.* **14** 3255
[51] Hołda A, Markowski R, Dębowska D, Kisiel A, Zimnal-Starnawska M, Piacentini M, Zema N and Lama F 1996 *Acta Phys. Pol.* A **90** 817
[52] Christman P, Meyer B K, Kreissl J, Schwarz R and Benz K W 1996 *Phys. Rev.* B **53** 3634
[53] Markowski R, Hołda A, Dębowska D, Kisiel A, Zimnal-Starnawska M, Piacentini M, Zema N and Lama F 1995 *Acta Phys. Pol.* A **88** 1023